

# Spectrally resolved hyperfine interactions between polaron and nuclear spins in organic light emitting diodes: Magneto-electroluminescence studies

S. A. Crooker,<sup>1</sup> F. Liu,<sup>2</sup> M. R. Kelley,<sup>1</sup> N. J. D. Martinez,<sup>1</sup> W. Nie,<sup>1</sup> A. Mohite,<sup>1</sup> I. H. Nayyar,<sup>1</sup> S. Tretiak,<sup>1</sup> D. L. Smith,<sup>1</sup> and P. P. Ruden<sup>2</sup>

<sup>1</sup>Los Alamos National Laboratory, Los Alamos, New Mexico 87545, USA

<sup>2</sup>University of Minnesota, Minneapolis, Minnesota 55455, USA

(Received 20 August 2014; accepted 8 October 2014; published online 17 October 2014)

We use spectrally resolved magneto-electroluminescence (EL) measurements to study the energy dependence of hyperfine interactions between polaron and nuclear spins in organic light-emitting diodes. Using layered devices that generate bright exciplex emission, we show that the increase in EL emission intensity  $I$  due to small applied magnetic fields of order 100 mT is markedly larger at the high-energy blue end of the EL spectrum ( $\Delta I/I \sim 11\%$ ) than at the low-energy red end ( $\sim 4\%$ ). Concurrently, the *widths* of the magneto-EL curves increase monotonically from blue to red, revealing an increasing hyperfine coupling between polarons and nuclei and directly providing insight into the energy-dependent spatial extent and localization of polarons. © 2014 AIP Publishing LLC. [<http://dx.doi.org/10.1063/1.4898700>]

Several recent experiments have shown that small applied magnetic fields  $\mathbf{B}$  on the order of 10–100 mT can induce substantial ( $\sim 10\%$ ) changes in the total light intensity emitted by organic light-emitting diodes (OLEDs).<sup>1–13</sup> While initially surprising in view of the fact that the polymers and small molecules used in OLEDs are primarily composed of non-magnetic atoms (H, C, and N), it was quickly appreciated that *hyperfine* spin interactions underpinned these phenomena. Specifically, the coupling of the electron and hole polaron spins to the many nuclear spins in the host material generates randomly oriented local effective magnetic fields about which electron and hole polaron spins can precess. This precession leads to spin mixing between singlet and triplet polaron-pair states, which are precursors to exciton or exciplex formation in an OLED. Applied fields  $\mathbf{B}$  suppress this hyperfine-induced mixing, altering the population balance between singlet and triplet excitons or exciplexes, which in turn modifies the electroluminescence (EL) efficiency.

The detailed dependence of EL intensity on  $\mathbf{B}$  allows direct insight into not only the rates of singlet and triplet exciton/exciplex formation but also reveals the strength of hyperfine coupling and therefore provides a measure of the spatial extent (size) of the electron and hole polarons.

In magneto-EL studies to date,<sup>1–13</sup> only the total (spectrally integrated) EL intensity was measured as a function of  $\mathbf{B}$ . However, OLED emission spectra typically span a very broad wavelength range, reflecting the fact that excitons and exciplexes form over a wide range of energies, and with varying degrees of localization for which different hyperfine couplings may be expected. Here, we spectrally resolve the magneto-EL from OLEDs based on 4,4',4''-tris(N-3-methylphenyl-N-phenylamino)triphenylamine (MTDATA) and 4,7,-diphenyl-1,10-phenanthroline (Bphen) a well known exciplex emitter—and show that the increase in EL intensity due to  $\mathbf{B}$  is significantly larger at the high-energy blue side of the spectrum than at the low-energy red side. Most importantly, the widths of the magneto-EL curves increase by over

a factor of two from blue to red, directly revealing an increasingly strong hyperfine coupling and providing insight into the energy-dependent spatial extent and localization of the emitting states.

Figure 1(a) depicts our layered OLED structures. They have transparent ITO/PEDOT anode contacts (indium tin oxide/polyethylenedioxythiophene), 50 nm thick hole transport layers of *m*-MTDATA, and 50 nm thick electron transport layers of Bphen. All active layers were deposited by thermal evaporation in vacuum ( $\sim 10^{-7}$  Torr). LiF/Al cathodes (1/100 nm) deposited by vacuum evaporation through a shadow mask produce OLEDs with 3.5 mm<sup>2</sup> area. The diagram shows the relative energy level alignments and depicts the bound electron/hole complex—the exciplex—that forms at the interface and which gives rise to EL. In contrast to an exciton (a bound electron-hole pair residing on the *same* molecule), an exciplex consists of electron and hole polarons localized predominantly on the different molecules (Bphen and MTDATA,

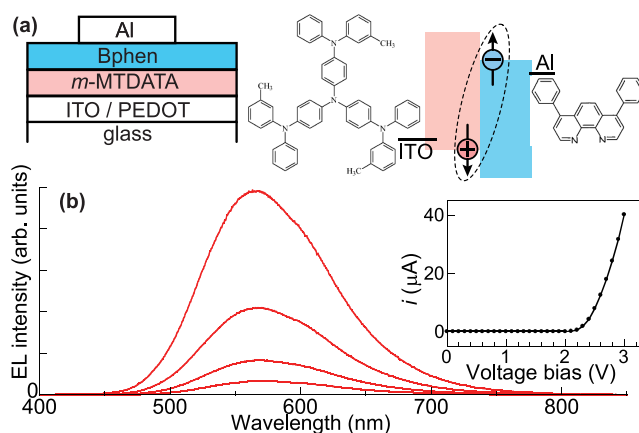


FIG. 1. (a) Schematic of the layered *m*-MTDATA/Bphen OLEDs. The diagram depicts the relative energy level alignments and the exciplex that forms at the interface. (b) Electroluminescence (EL) spectra at 32, 16, 8, and 4  $\mu\text{A}$  current bias (300 K,  $\mathbf{B} = 0$ ). Inset: typical current-voltage behavior.

respectively), giving the excitation a pronounced charge-transfer character.

The OLEDs were measured in vacuum at room temperature. Typical current-voltage curves exhibit the expected diode-like behavior and low turn-on voltage [inset of Fig. 1(b)]. EL spectra were measured by a 300 mm spectrometer and a charge coupled device (CCD) detector. Fig. 1(b) shows typical EL spectra acquired in zero magnetic field, at different bias currents. The EL extends across the visible spectrum from 450 to 750 nm and is peaked at  $\sim 570$  nm. Owing to the relative energy level alignments of MTDATA and Bphen, EL is expected to originate solely from radiative recombination of exciplexes. The measured EL spectra are consistent with exciplex emission, and importantly, no emission is observed from excitons in the MTDATA or Bphen materials themselves (which would otherwise occur at shorter wavelengths in the 350–450 nm range<sup>14,15</sup>), indicating the absence of unipolar currents across the heterojunction in these OLEDs. The EL spectra are in good agreement with the previous studies of related exciplex-emitting OLEDs based on these materials.<sup>14–18</sup>

Small magnetic fields  $\mathbf{B}$  clearly increase the total EL emission intensity in these devices, as shown in Fig. 2(a). Figure 2(b) shows the detailed dependence of the EL

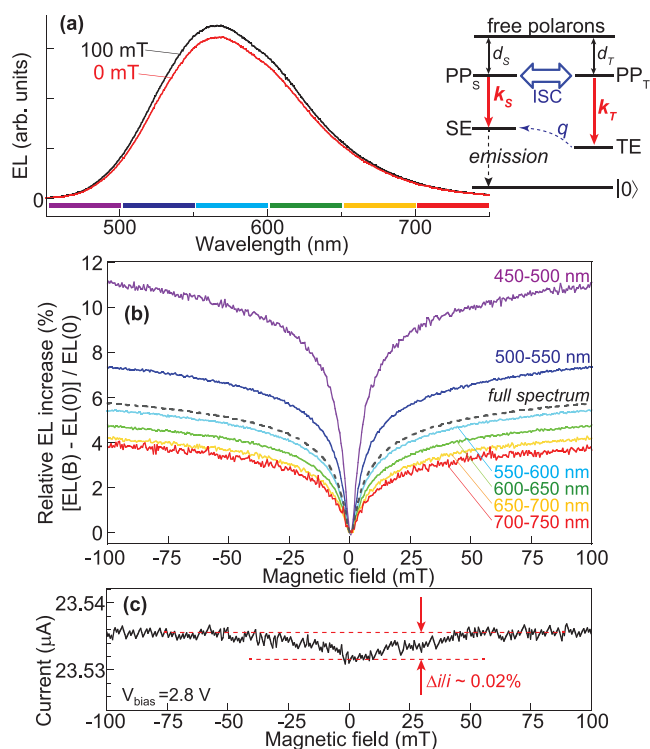


FIG. 2. (a) EL spectra at  $\mathbf{B}=0$  and 100 mT. Inset: Exciplex formation model. Weakly bound singlet and triplet polaron pairs (PP) form from free carriers. Intersystem crossing (ISC) between  $PP_S$  and  $PP_T$  exists at  $\mathbf{B}=0$  due to hyperfine coupling to randomly oriented nuclear spins. Singlet and triplet exciplexes (SE, TE) subsequently form with rates  $k_S$  and  $k_T$ . A fraction  $q$  of TE states may undergo thermally activated ISC to SE states ( $0 < q < 1$ ). Only SE recombines radiatively. (b) The relative EL intensity versus  $\mathbf{B}$ , integrated over the wavelengths indicated. At blue wavelengths, the  $\mathbf{B}$ -induced EL increase is larger (indicating larger  $k_T/k_S$  ratio, or smaller  $q$ ), and the curves are narrower (indicating weaker hyperfine coupling, due to larger polarons at these energies). The dashed line indicates the total (spectrally integrated) EL. (c) The OLED resistance does not vary significantly with  $\mathbf{B}$ .

intensity on  $\mathbf{B}$ . Note first the dashed black curve labeled “full spectrum,” which shows that the total (spectrally integrated) EL intensity grows with  $|\mathbf{B}|$  by  $\sim 6\%$  at  $\pm 100$  mT. These overall trends are consistent with recent studies of magneto-EL phenomena in various polymer and small-molecule based OLEDs.<sup>1–13</sup> The origin of this effect is believed to lie in the suppression by  $\mathbf{B}$  of the mixing between singlet and triplet polaron-pairs, which form as an initial step in the exciplex formation process. Importantly, the depth and width of these magneto-EL curves shown in Fig. 2(b) provide insight into the relative rates of singlet and triplet exciplex formation, and also provide a measure of the hyperfine coupling strength between the polaron spins and the underlying nuclear spins of the molecules, as described in the following:

These data can be understood in the context of the diagram in Fig. 2(a), which we adapt to our MTDATA/Bphen OLEDs from the previous descriptions by, e.g., Ehrenfreund<sup>12</sup> and Kersten<sup>11</sup> and the excellent discussions contained therein. In our OLEDs, free electron and hole carriers (polarons) are injected at the contacts, and these drift to the MTDATA/Bphen interface. Coulomb attraction leads initially to the formation of very weakly bound polaron-polaron (PP) pairs, which can form as either spin-singlets or spin-triplets ( $PP_S$ ,  $PP_T$ ). At this stage, the polarons are well-separated and electron-hole exchange interactions are negligible, so that  $PP_S$  and  $PP_T$  states have the same energy.

Hyperfine coupling of the electron and hole polaron spins to the underlying “bath” of randomly oriented nuclear spins on each molecule (primarily spin- $\frac{1}{2}$   $^1\text{H}$ ) leads to precession of the electron and hole spins about an effective (Overhauser) magnetic field  $\mathbf{B}_{\text{hf}}$ . Importantly, the magnitude and orientation of  $\mathbf{B}_{\text{hf}}$  are different on every molecule. The independent spin precession of the electron and hole therefore causes a spin mixing (or “intersystem crossing,” ISC) between the degenerate  $PP_S$  and  $PP_T$  states. From these weakly bound states, more strongly bound singlet and triplet exciplexes (SE and TE) can form with rates  $k_S$  and  $k_T$ . It can be convenient to consider this last step in the exciplex-formation process as the electron (hole) polaron hopping to the Bphen (MTDATA) molecule that is closest to the hole (electron) polaron.<sup>11</sup> The polarons now overlap sufficiently to generate a significant exchange splitting  $\Delta_{ST}$  between SE and TE states (estimated to be 10–100 meV; see below), which greatly exceeds the small Zeeman energy from  $\mathbf{B}_{\text{hf}}$  ( $E_Z \sim 2 \mu\text{eV}$  if  $|\mathbf{B}_{\text{hf}}| = 20$  mT). Therefore, SE-TE mixing due to  $\mathbf{B}_{\text{hf}}$  alone is extremely weak. It was recently suggested,<sup>18</sup> however, from studies of related exciplex emitters that some fraction  $q$  of long-lived TE states may undergo thermally activated ISC to SE states, a process also considered (see diagram). This fraction  $q$  is unaffected by magnetic fields to leading order, again because  $E_Z \ll \Delta_{ST}$ . This model assumes that only singlet exciplexes recombine radiatively.

$\mathbf{B}_{\text{hf}}$  can be estimated from the sum of hyperfine energies from the random nuclear spins:  $\sum_k a_k \mathbf{S} \cdot \mathbf{I}_k |\Psi(\mathbf{r}_k)|^2$ , where  $\mathbf{S}$  and  $\mathbf{I}_k$  are the polaron and nuclear spin,  $a_k$  is the hyperfine coupling constant, and  $\Psi(\mathbf{r}_k)$  is the polaron wavefunction at the  $k$ th nucleus. Averaging over many polarons, the rms amplitude of  $\mathbf{B}_{\text{hf}} \sim 1/\sqrt{N} \sim 1/\sqrt{V}$ , where  $N$  is the number of nuclei within the polaron wavefunction,<sup>10</sup> which has characteristic volume  $V$ .

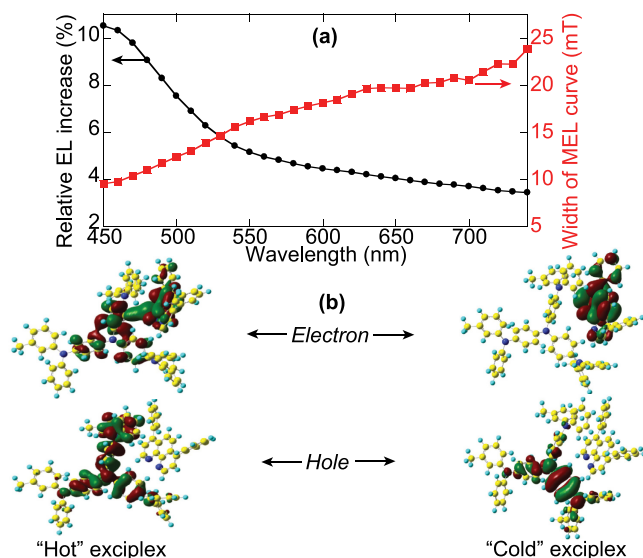


FIG. 3. (a) Left axis (circles): The relative increase in EL intensity due to  $\mathbf{B}$  (i.e., the “depth” of the curves shown in Fig. 2(b)), versus EL wavelength. Short (blue) wavelengths show the largest change indicating larger  $k_T/k_S$  ratios and/or smaller  $q$ . Right axis (squares): The corresponding full width of the magneto-EL curves ( $\propto 2|\mathbf{B}_{\text{hf}}|$ ).  $\mathbf{B}_{\text{hf}}$  is smaller at blue wavelengths, indicating more delocalized (larger) polarons. (b) Natural transition orbitals of an electron and hole, calculated for “hot” (unrelaxed) and “cold” (vibrationally relaxed) exciplexes on a MTDATA/Bphen molecular pair.

Crucially, if (and only if) the exciplex formation rates  $k_S$  and  $k_T$  are unequal, then any process that influences the  $\text{PP}_S$  -  $\text{PP}_T$  mixing will change the balance between SE and TE populations and will therefore affect the EL intensity. Applied fields  $\mathbf{B}$  provide one such route: If  $|\mathbf{B}| \gg |\mathbf{B}_{\text{hf}}|$ , then the net magnetic fields “seen” by the electron and hole in a polaron-pair are no longer random but are both  $\approx \mathbf{B}$ . The polarons therefore precess in synchrony (if their  $g$ -factors are similar), and  $\text{PP}_S$ - $\text{PP}_T$  mixing is suppressed. The characteristic half-widths of the magneto-EL curves in Fig. 2(b) indicate when  $|\mathbf{B}| \sim |\mathbf{B}_{\text{hf}}|$ , thereby providing a measure of the hyperfine coupling strength in these molecules. Moreover, the *depth* of the curves is influenced by the exciplex formation ratio  $k_T/k_S$  and by the fraction  $q$ .

Magneto-EL studies to date have considered only the field dependence of the *total* (spectrally integrated) EL,<sup>1-13</sup> shown here for our OLEDs by the dashed line in Fig. 2(b). However, our spectrally resolved data reveal a significant difference in both the depth and width of the magneto-EL data as

a function of EL wavelength. As shown in Fig. 2(b),  $\mathbf{B}$  induces a much larger EL boost at the blue end of the EL spectrum ( $\sim 11\%$ ) as compared to the red end ( $\sim 4\%$ ). (These values are independent of field direction.) It is also evident that the *widths* of the magneto-EL curves vary significantly across the EL spectrum. They are narrower at blue wavelengths, indicating smaller  $\mathbf{B}_{\text{hf}}$  for exciplexes that form at high energies. Since the rms magnitude of  $\mathbf{B}_{\text{hf}} \propto 1/\sqrt{V}$  as discussed above, this directly provides information about the localization and effective “size” of the polaron wavefunctions.

We note that the large EL changes are not simply due to magneto-resistive effects that can occur in organic materials.<sup>19,20</sup> Figure 2(c) shows the simultaneously measured current through the OLED, which changes only slightly (0.02%). Therefore, to leading order,  $\mathbf{B}$  influences primarily the radiative exciplex recombination rate but not the total recombination rate.

Figure 3(a) summarizes these trends by showing the spectrally resolved depth and width of the magneto-EL data. The depth drops rapidly across the blue-green part of the EL spectrum (450–550 nm) and falls to one-third of its maximum value by 750 nm. This trend indicates that the exciplex formation ratio  $k_T/k_S$  decreases towards unity across the spectrum and/or that  $q$  increases, as discussed below. Concurrently, the width of the magneto-EL curves increases steadily across the spectrum and approximately doubles in value, suggesting that the characteristic volume  $V$  of the polaron wavefunctions in low-energy exciplexes has shrunk four-fold.

To visualize the polaron wavefunctions, we performed electronic structure calculations of a Bphen/MTDATA molecular pair. An optimal ground state geometry was obtained using Density Functional Theory (DFT), and electronic excitations and excited geometries were calculated using time-dependent DFT.<sup>21-24</sup> Figure 3 shows natural transition orbitals<sup>25</sup> of an electron and hole for an unrelaxed (higher energy, or “hot”) exciplex and also for a vibrationally relaxed (lower energy, or “cold”) exciplex. In the former case, the wavefunctions are more spatially extended and have some overlap due to partial delocalization of the electron between Bphen and MTDATA, which will generate larger SE-TE exchange splitting  $\Delta_{ST}$ . In the latter case, the wavefunctions are more localized on their respective molecules. Estimates of  $\Delta_{ST}$  range from 10 to 100 meV given the uncertainty of molecular orientations and the choice of DFT model.

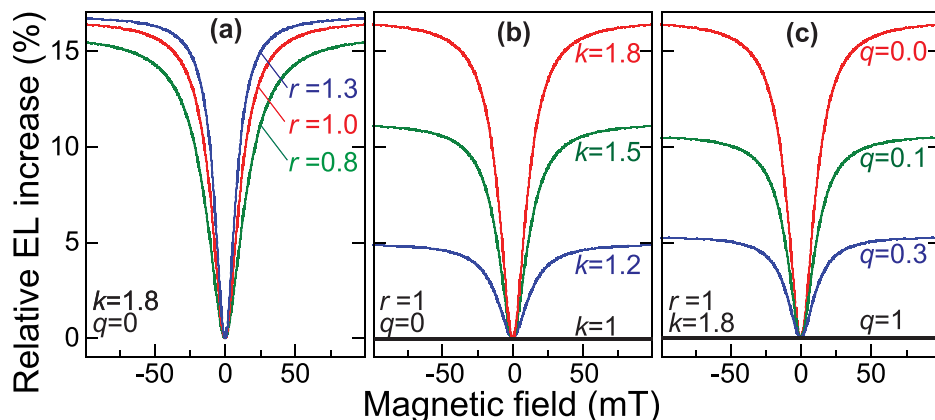


FIG. 4. Modeling the magneto-EL. The key parameters are the normalized lengthscale  $r$  of the polaron wavefunction, the ratio of exciplex formation rates  $k = k_T/k_S$ , and the fraction  $q$ . The characteristic hyperfine field  $\mathbf{B}_{\text{hf}} \propto 1/\sqrt{V} \propto r^{-3/2}$ .

To model the magneto-EL data analytically, we employed a density matrix model for the ensemble of electron and hole polaron spins in the PP states, including Zeeman terms and hyperfine interactions with randomly oriented  $^1\text{H}$  nuclei. The time evolution of the density matrix is described by a stochastic Liouville equation.<sup>11</sup> Steady-state analytical solutions are obtained using Bloch-Wangsness-Redfield theory.<sup>26</sup> As polarons hop between different molecules, they experience fluctuating  $\mathbf{B}_{\text{hf}}$ . The resulting SE and TE densities are calculated from the corresponding PP density matrix elements, the exciplex formation rates  $k_T$  and  $k_S$ , and the fraction  $q$  of TE states undergoing thermally activated ISC to SE states.

Three key parameters control the shape of the calculated magneto-EL curves, which are determined from the relative SE density: the spatial extent of the polarons as characterized by a normalized length  $r$ , the ratio  $k = k_T/k_S$ , and  $q$ . All parameters may vary locally due to random steric interactions between the molecules. The model allows for different spin-spin correlation functions, with the simplest being a single exponential decay which yields inverted-Lorentzian curves when  $k > 1$ . In Figs. 4(a)–4(c),  $r$ ,  $k$ , and  $q$  are varied, while the other two parameters are fixed, respectively. The width of the magneto-EL curves is principally determined by  $r$ , while  $k$  and  $q$  act primarily as overall scaling factors that determine the “depth” of the curves. More localized polarons (smaller  $r$ , and therefore larger  $\mathbf{B}_{\text{hf}}$ ) are associated with EL at longer wavelengths, while delocalized polarons are associated with short-wavelength EL. Overall, the calculated line shapes and trends are consistent with experimental data.

In summary, spectrally resolved magneto-EL measurements provide considerable insight into the energy-dependent exciplex formation rates and hyperfine interactions in OLEDs, both of which depend in turn on the localization and detailed spatial extent of the electron and hole polarons themselves. We anticipate that similarly valuable information can be obtained for situations where light emission derives from excitons in single-component OLEDs.

This work was supported by the Los Alamos LDRD program and by NSF MRSEC DMR-0819885.

- <sup>1</sup>J. Kalinowski, M. Cocchi, D. Virgili, P. DiMarco, and V. Fattori, *Chem. Phys. Lett.* **380**, 710 (2003).
- <sup>2</sup>A. H. Davis and K. Bussmann, *J. Vac. Sci. Technol. A* **22**, 1885 (2004).
- <sup>3</sup>Y. Sheng, T. D. Nguyen, G. Veeraraghavan, Ö. Mermer, M. Wohlgenannt, S. Qiu, and U. Scherf, *Phys. Rev. B* **74**, 045213 (2006).
- <sup>4</sup>Y. Iwasaki, T. Osasa, M. Asahi, M. Matsumura, Y. Sakaguchi, and T. Suzuki, *Phys. Rev. B* **74**, 195209 (2006).
- <sup>5</sup>H. Odaka, Y. Okimoto, T. Yamada, H. Okamoto, M. Kawasaki, and Y. Tokura, *Appl. Phys. Lett.* **88**, 123501 (2006).
- <sup>6</sup>Y. Wu, Z. Xu, B. Hu, and J. Howe, *Phys. Rev. B* **75**, 035214 (2007).
- <sup>7</sup>P. Desai, P. Shakya, T. Kreouzis, W. P. Gillin, N. A. Morley, and M. R. J. Gibbs, *Phys. Rev. B* **75**, 094423 (2007).
- <sup>8</sup>F. J. Wang, H. Bässler, and Z. V. Vardeny, *Phys. Rev. Lett.* **101**, 236805 (2008).
- <sup>9</sup>B. Hu, L. Yan, and M. Shao, *Adv. Mater.* **21**, 1500 (2009).
- <sup>10</sup>T. D. Nguyen, G. Hukic-Markosian, F. Wang, L. Wojcik, X. G. Li, E. Ehrenfreund, and Z. V. Vardeny, *Nat. Mater.* **9**, 345 (2010).
- <sup>11</sup>S. P. Kersten, A. J. Schellekens, B. Koopmans, and P. A. Bobbert, *Phys. Rev. Lett.* **106**, 197402 (2011).
- <sup>12</sup>E. Ehrenfreund and Z. V. Vardeny, *Isr. J. Chem.* **52**, 552 (2012).
- <sup>13</sup>T. D. Nguyen, T. P. Basel, Y.-J. Pu, X.-G. Li, E. Ehrenfreund, and Z. V. Vardeny, *Phys. Rev. B* **85**, 245437 (2012).
- <sup>14</sup>D. Wang, W. Li, B. Chu, Z. Su, D. Bi, D. Zhang, J. Zhu, F. Yan, Y. Chen, and T. Tsuboi, *Appl. Phys. Lett.* **92**, 053304 (2008).
- <sup>15</sup>F. Yan, R. Chen, H. Sun, and X. W. Sun, *Appl. Phys. Lett.* **104**, 153302 (2014).
- <sup>16</sup>D. Virgili, M. Cocchi, V. Fattori, C. Sabatini, J. Kalinowski, and J. A. G. Williams, *Chem. Phys. Lett.* **433**, 145 (2006).
- <sup>17</sup>P. Chen, Q. Peng, L. Yao, N. Gao, and F. Li, *Appl. Phys. Lett.* **102**, 063301 (2013).
- <sup>18</sup>K. Goushi, K. Yoshida, K. Sato, and C. Adachi, *Nat. Photonics* **6**, 253 (2012).
- <sup>19</sup>W. Wagemans, P. Janssen, A. J. Schellekens, F. L. Bloom, P. A. Bobbert, and B. Koopmans, *SPIN* **1**, 93 (2011).
- <sup>20</sup>N. J. Harmon and M. Flatté, *Phys. Rev. B* **85**, 075204 (2012).
- <sup>21</sup>We used wB97XD/6-31G\* model chemistry. wB97XD is a range-corrected functional with empirical London dispersion terms, allowing to describe excitons, charge-transfer states, and weakly van-der-Waals bound complexes. Simulations used Gaussian 09 software.
- <sup>22</sup>J.-D. Chai and M. Head-Gordon, *Phys. Chem. Chem. Phys.* **10**, 6615 (2008).
- <sup>23</sup>R. J. Magyar and S. Tretiak, *J. Chem. Theory Comput.* **3**, 976 (2007).
- <sup>24</sup>S. Grimme, *Comp. Mol. Sci.* **1**, 211 (2011).
- <sup>25</sup>R. L. Martin, *J. Chem. Phys.* **118**, 4775 (2003).
- <sup>26</sup>C. P. Slichter, *Principles of Magnetic Resonance*, 3rd ed. (Springer, UIUC, IL, USA, 1990).